

A Catalytic and Shape-Memory Polymer Reactor

Yanli Han, Xinhua Yuan, Maiyong Zhu, Songjun Li,* Michael J. Whitcombe, and Sergey A. Piletsky

An originally designed catalytic and shape-memory polymer reactor is reported. This reactor is made of a unique shape-switchable polymer composed of a thermosensitive control layer and an inert substrate layer. With the inert substrate layer made of poly(acrylamide), the thermosensitive control layer consists of nickel nanoparticles and a smart polymer composite of poly(1-vinylimidazole) (PVIIm) and poly(acrylic acid) (PAAc) that exhibit switchable domains. The self-healing and dissociation between PVIIm and PAAc induce convex/concave-switchable shapes in the resulting reactor, which cause tunable access to the encapsulated metal nanoparticles. In this way, this reactor demonstrates tunable catalytic ability. Unlike reported smart polymer reactors exhibiting tunable catalysis usually due to the thermal phase transition of poly(*N*-isopropylacrylamide) (PNIPAm), this novel reactor adopts the shape-switchable strategy for tunable catalysis. This novel design suggests a new protocol for the development of smart catalytic reactors, which opens new opportunities for controlled chemical processes.

catalytic reactors cannot find practical applications, mainly because most of the reported polymers that are suitable for supporting metal nanoparticles are not PNIPAm,^[5–7] which lack thermal phase transition and thus adjustable elements. Furthermore, from a practical point of view it is complicated and challenging to identify the polymers' hydrophilic and/or hydrophobic properties during the catalytic process. Thus, more protocols and in particular new protocols are urged.

For centuries, mankind has been learning and achieving knowledge from nature. A body of knowledge is already available. One of them is the shape-memory polymers (SMPs),^[8] which appear to provide a promising prospect for catalytic reactors. Although the SMPs and their mechanisms are diverse, the common ground lies in the conceptual

combination of static netpoints that stabilize the permanent shape and dynamic switching domains fixing the temporary shape. The change in chain mobility upon temperature in the switching domains is the major driving force that transforms a temporary shape to the permanent shape.^[9] These SMPs can perform even more complex shape changes when prepared in a two- or multi-layer form composed of control layers and substrate layers. By using PNIPAm as the control layer and poly(acrylamide) as the substrate layer, the resulting polymer was found capable of switching between an arch and a concave shape.^[10] It is even possible to obtain spiral, cylindrical, wavy, and ribbon-like structures based on SMPs consisting of several alternating layers.^[11,12] The change in shape is reversible and these systems can switch between two or more defined shapes by depending upon the temperature (whether it is below or above the transition temperature), which thereby avoids the need for external mechanical manipulation. In this way, these SMPs demonstrate the multi-way shape memory effects. Although these works are not directly related to catalytic applications, the methods developed by SMP scientists provide new insight into the stranded catalytic reactors, which makes feasible the switchable domains.

Inspired by this principle, we herein report a unique catalytic and shape-memory polymer reactor (**Scheme 1**). In order to avoid external mechanical manipulation and the need for PNIPAm, as well as to control the reactor in an on/off-switchable way upon changing temperature, this reactor was fabricated in a two-layer form composed of a thermosensitive control layer and an inert substrate layer. With the inert substrate

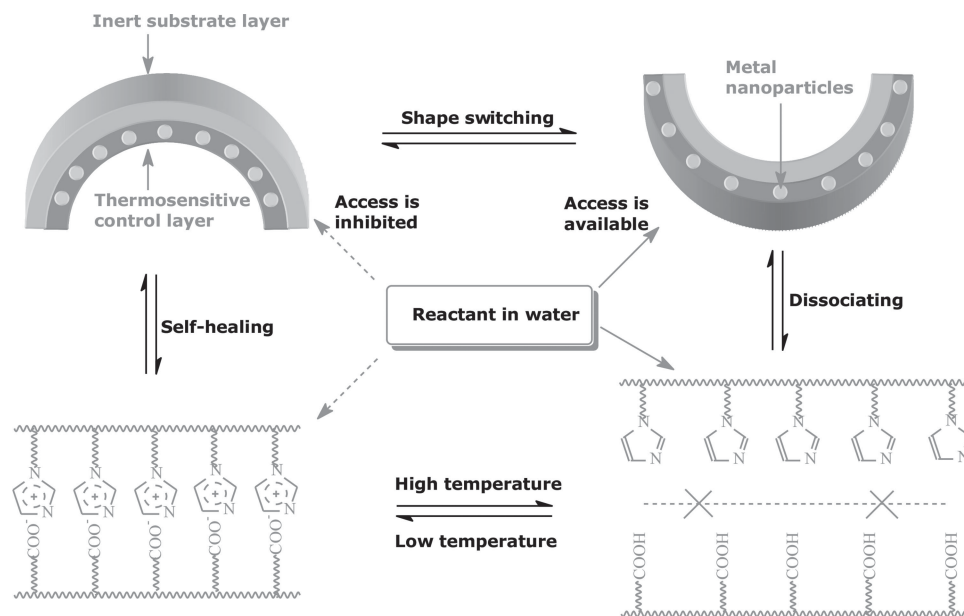
1. Introduction

Metal nanoparticles are of great importance in a broad range of applications and in particular in catalytic applications. The recent advances in this field and advanced materials offer new opportunities to develop functional catalysts by incorporating both of them into individual entities.^[1,2] Prominent among them are the so-called smart catalytic reactors, which gain traction due to the tantalizing demand for controlled processes in chemical synthesis and in inaccessible places. With the earliest endeavors made in developing poly(*N*-isopropylacrylamide) (PNIPAm)-encapsulated Ag nanoparticles,^[3,4] the reactors demonstrate tunable catalysis in water, resulting from the thermal phase transition of PNIPAm. The relative balance between the hydrophilic and the hydrophobic properties in the polymer causes either an impeded or an unobstructed access into the encapsulated Ag nanoparticles. In this way, catalysis by the reactors is recognized as a tunable process. Nonetheless, such

Y. Han, Prof. X. Yuan, Dr. M. Zhu, Prof. S. Li
School of Materials Science & Engineering
Jiangsu University
Zhenjiang 212013, China
E-mail: Lsjchem@ujs.edu.cn
Dr. M. J. Whitcombe, Prof. S. A. Piletsky
Department of Chemistry
University of Leicester
Leicester LE1 7RH, UK



DOI: 10.1002/adfm.201400768



Scheme 1. Proposed mechanism for the NiPR-S reactor.

layer made of poly(acrylamide), the thermosensitive control layer consisted of nickel nanoparticles and a unique polymer composite of poly(1-vinylimidazole) (PVI_m) and poly(acrylic acid) (PAAc) that exhibited switchable domains.^[13] As outlined in Scheme 1, this polymer reactor (i.e., “NiPR-S”) was capable of tunable catalysis due to the switchable domains. The self-healing and dissociation between PVI_m and PAAc caused convex/concave- switchable shapes in the resulted reactor, which thus caused tunable access to the encapsulated metal nanoparticles. In this way, catalysis by this reactor demonstrated a tunable way. For a comparative study, two controls, i.e., “NiPR-N” and “PR-S”, were also prepared under comparable conditions. NiPR-N was the non-responsive nickel reactor prepared using poly(acrylamide) in both layers (herein “N” means the non-responsive feature in contrast to the “S” switchable properties in SMPs). PR-S was the polymeric carrier of NiPR-S and prepared without using nickel. The objective of this study is to demonstrate that catalytic reactors with self-switchable ability can be fabricated by using this novel design, which suggests new opportunities for controlled chemical processes.

2. Results and Discussion

2.1. Characterization of Composition and Structure

This novel polymer reactor was fabricated in a two-layer form composed of a thermosensitive control layer and an inert substrate layer. The thermosensitive control layer was first prepared by polymerization and then exposed with one side to an aqueous solution of acrylamide, which allowed for the formation of the substrate layer.^[14] Thus, this reactor was composed of the poly(acrylamide) layer and one unique thermosensitive layer, which consisted of nickel nanoparticles and the supporting polymer composite of PVI_m and PAAc.

Fourier transform infrared spectroscopy (FTIR) was first used to characterize the composition in both layers. As shown in Figure 1, three major bands (3000–3500, 1500–1750, and 1000–1500 cm⁻¹) appeared in both layers. These bands were complex due to the complicated composition, which may be associated with the stretching of O-H/N-H, C=O, and C-N/C-C.^[15] For a comparative study, we also included the FTIR spectra of two controls in Figure 1. As expected, PR-S exhibited almost the same spectrum as NiPR-S whereas

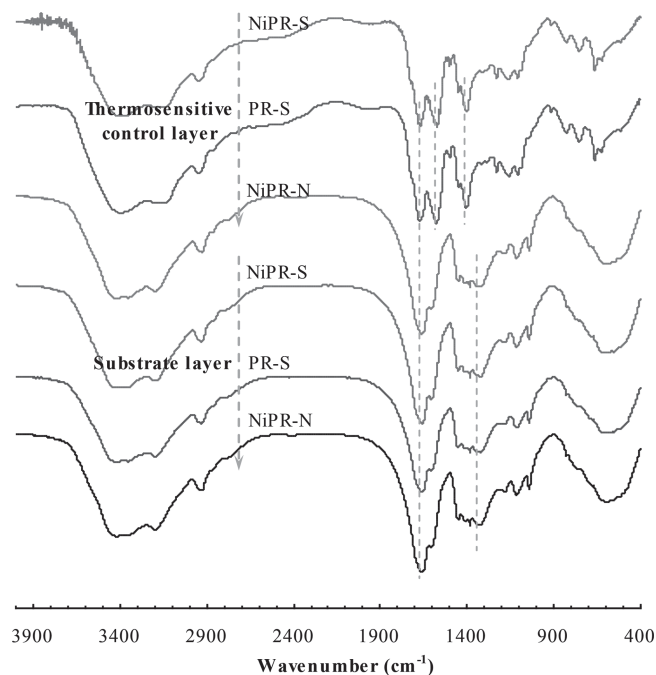


Figure 1. FTIR spectra of both the control and the substrate layers contained in the prepared polymer reactors.

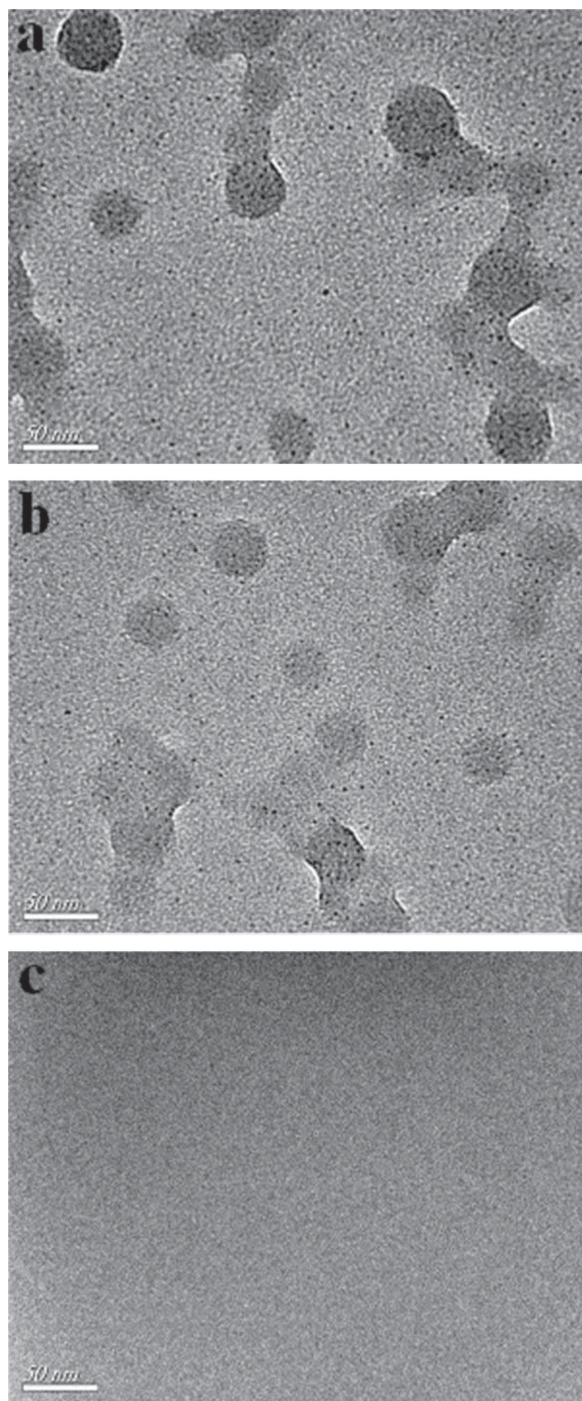


Figure 2. TEM images of metal nanoparticles contained in the prepared polymer reactors (a: NiPR-S; b: NiPR-N; c: PR-S).

NiPR-N failed to. Both NiPR-S and PR-S showed one strong absorption peak at $1500\text{--}1750\text{ cm}^{-1}$ in contrast to NiPR-N. This result may be due to the comparable composition of PR-S and the supporting polymer of NiPR-S. The supporting polymer of NiPR-N did not contain PAAc and thus no absorption peak of the carbonyl groups in PAAc was observed. **Figure 2** shows transmission electron microscopy (TEM) images. Nickel nanoparticles with a size of ca. 40 nm were encapsulated in the

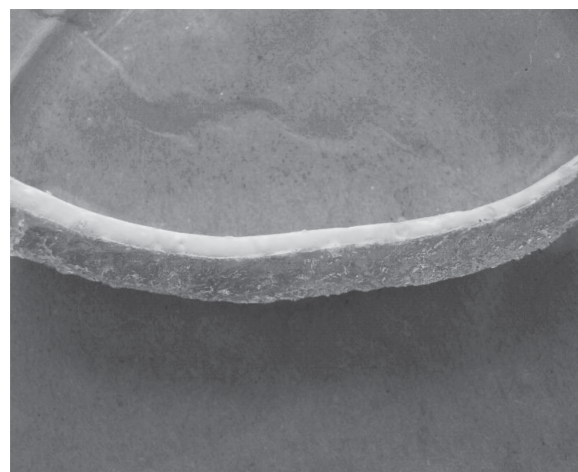


Figure 3. Digital picture in the outward appearance of a slice of NiPR-S.

polymeric building blocks. **Figure 3** presents the digital picture of NiPR-S which shows that the reactor has the expected two-layer structure. Thus, the reactors were prepared in the desired form.

2.2. Shape-Memory Effect and Switchable Interaction

Figure 4 displays the shape change of NiPR-S upon changing temperature. The slice of NiPR-S appeared to be convex at $50\text{ }^{\circ}\text{C}$, approximately flat at $40\text{ }^{\circ}\text{C}$ and concave at or below $25\text{ }^{\circ}\text{C}$. The change in shape is reversible and this system can switch between an arch and a concave shape upon changing temperature. As expected, NiPR-S demonstrated a shape-memory effect. The shape-memory effect, as previously explained, can be related to the self-switchable domains within NiPR-S. In contrast to the inert substrate layer, the self-healing and dissociation between PVI_m and PAAc caused swelling and

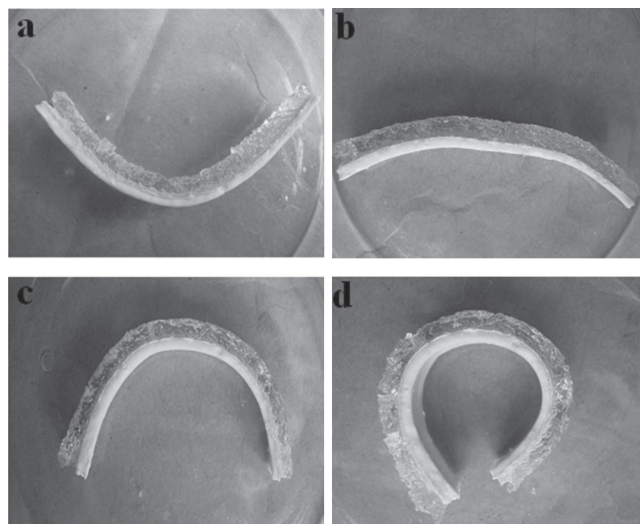


Figure 4. The shape change of NiPR-S upon changing temperature (a: $50\text{ }^{\circ}\text{C}$; b: $40\text{ }^{\circ}\text{C}$; c: $25\text{ }^{\circ}\text{C}$; d: $15\text{ }^{\circ}\text{C}$).

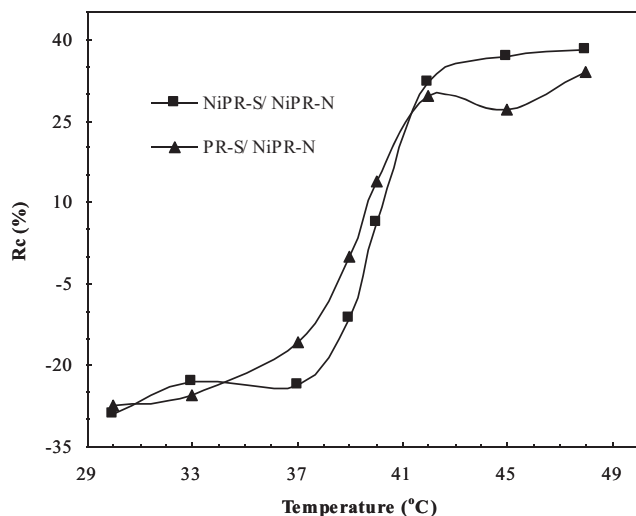


Figure 5. DLS curves of the thermosensitive layers contained in the prepared reactors.

shrinking of the control layer, which thereby induced a shape change in this reactor.

To address the PVIm-PAAc interaction, dynamic light scattering (DLS) was used to evaluate these polymer reactors.^[16] In order to reach equilibrium, all samples scraped from the thermosensitive layers of these reactors were kept at specified temperatures for at least 10 min before acquiring the hydrodynamic radius. By a comparison between the smart reactors (i.e., NiPR-S and PR-S) and the non-responsive NiPR-N, the contribution of the PVIm-PAAc interaction is thus reflected in the change of the hydrodynamic radius (R_c). As shown in **Figure 5**, the R_c of NiPR-S revealed a significant dependence upon temperature, in contrast to NiPR-N. The R_c of NiPR-S increased with elevated temperature and the major change appeared at ca. 40 °C. Below 40 °C, NiPR-S exhibited a low R_c associated with the self-healing between PVIm and PAAc, which inhibited the swelling of the polymer. In contrast, above 40 °C, the R_c of NiPR-S dramatically increased in response to the dissociation of the PVIm-PAAc interaction, which caused a swelling of the polymer. This result suggests that the shape change of NiPR-S was a result of the self-switchable interaction between PVIm and PAAc.

2.3. Switching Catalysis

The catalytic properties of these polymer reactors were evaluated using the reduction of sodium fluorescein in the presence of sodium borohydride.^[17] As shown in **Figure 6**, PR-S did not reveal significant catalysis due to the lack of catalytic nickel nanoparticles. In contrast, NiPR-S and NiPR-N demonstrated significant catalytic ability, where the conversion increased rapidly with time. To verify the switching catalysis, two representative temperatures, 25 and 50 °C (either lower or higher than the transition temperature of NiPR-S, i.e., 40 °C), were selected for a comparative study. At 50 °C, NiPR-S revealed a significantly higher reactivity than NiPR-N. In contrast, at 25 °C, the catalytic activity in NiPR-S became lower than that

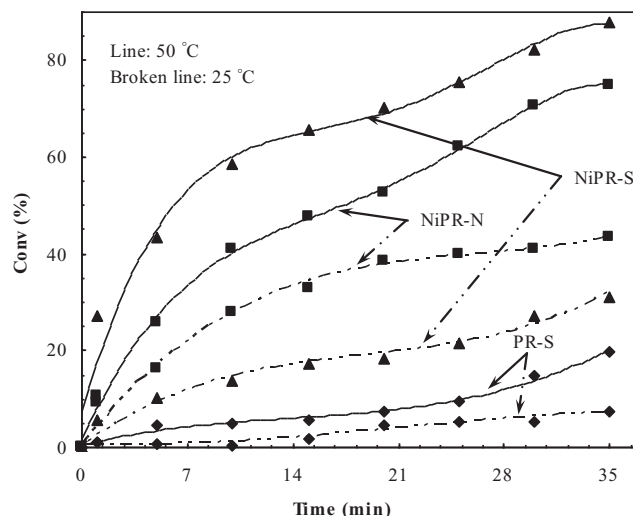


Figure 6. Catalytic activity of the prepared polymer reactors.

in NiPR-N. NiPR-S demonstrated the switching catalytic ability, as expected.

2.4. Access-Regulating Behavior

Electrochemical tests were further employed to achieve information on the tunable mechanism within the prepared polymer reactors.^[18] Using an electrochemical workstation, the Pt wire encircled by a thin film of the thermosensitive layers was adopted as the working electrode in a conventional three-electrode configuration. The redox process of $\text{HPO}_4^{2-}/\text{H}_2\text{PO}_4^-$ was used as a probe to achieve the current change upon changing temperature. By a comparison between the smart reactors (i.e., NiPR-S and PR-S) and the non-responsive NiPR-N, the effect of the thermosensitive interaction on the access to the polymer inner was thus exposed. As shown in **Figure 7**, the electrochemical system with electrodes modified by NiPR-S and PR-S exhibited a significant dependence upon temperature. In contrast, no significant change in current was observed in the system with electrodes modified by NiPR-N. This result indicates that the presence of PVIm-PAAc caused tunable access to the polymer inner of NiPR-S and PR-S. In conjunction with the catalytic study (**Figure 6**), this result further suggests that the thermosensitive interaction between PVIm and PAAc caused tunable access to the encapsulated metal nanoparticles, which thereby made feasible the switching catalysis.

3. Conclusions

A novel catalytic and shape-memory polymer reactor is reported in this study. This reactor was made of a unique shape-switchable polymer composed of a thermosensitive control layer and an inert substrate layer. The thermosensitive control layer consisted of nickel nanoparticles and a smart polymer composite of poly(1-vinylimidazole) and poly(acrylic acid) that exhibited switchable domains. The self-healing and dissociation of the

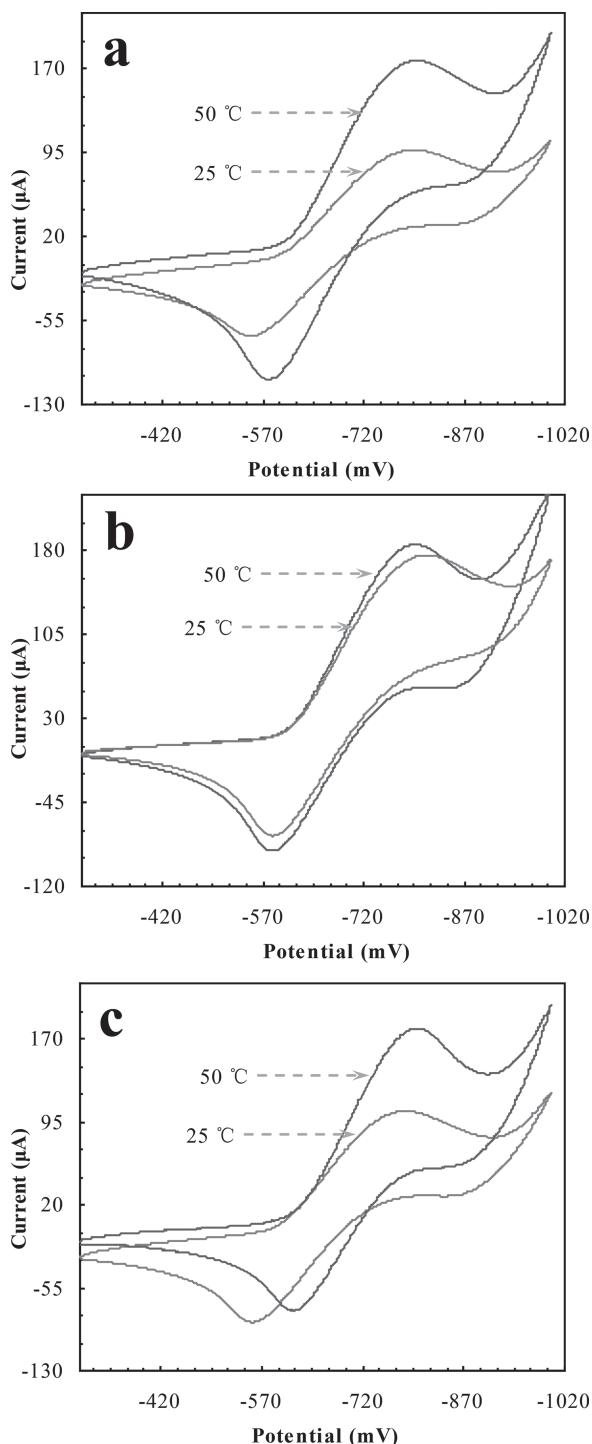


Figure 7. Cyclic voltammetry (CV) profiles with tunable access to the polymer inner of the prepared reactors (a: NiPR-S; b: NiPR-N; c: PR-S).

PVIm-PAAc interaction induced convex/concave-switchable shapes in the resulting reactor, which allowed tunable access to the encapsulated metal nanoparticles. At relatively low temperatures (such as 25 °C), this reactor appeared in an arch and exhibited weak catalytic ability due to the self-healing between PVIm and PAAc, which inhibited access to the encapsulated

metal nanoparticles. In contrast, at relatively high temperatures (such as 50 °C), this reactor appeared in a concave shape and revealed significant catalysis, resulting from the dissociation of the PVIm-PAAc interaction. It is thus suggested that non-PNIPAm reactors with self-switchable catalytic ability can be developed by using this novel design, which opens new opportunities in controlled chemical processes. Future development in this field will significantly increase the potential for applications, and will lead to the appearance of novel catalytic materials and functional catalysts.

4. Experimental Section

Preparation of Polymer Reactors: The chemicals used were of analytic grade and used as received from Sigma-Aldrich. The polymer reactor, as previously discussed, was fabricated in a two-layer form composed of a thermosensitive control layer and an inert substrate layer. The thermosensitive control layer was first prepared using the polymerization system described below. To connect the two different layers,^[11,12,14] one side of the control layer was then exposed to an aqueous solution of acrylamide. In this way, the acrylamide solution diffused into the control layer for a certain time. The acrylamide was then polymerized by the addition of a radical initiator to form an interpenetrating network. In detail, the control layer was prepared using a polymerization system including 1-vinylimidazole (1.41 g), acrylic acid (1.08 g), ammonium persulphate (0.07 g), and methylenebisacrylamide (2 wt%), along with nickel nitrate hexahydrate (0.48 g), which were dissolved in dimethyl sulfoxide (3 mL). After this system was dispersed and deoxygenated via sonication and nitrogen, the mixture system was irradiated with ultraviolet light (365 nm) overnight. The encapsulated nickel ions were then reduced by an excess of sodium borohydride (tenfold, with regard to ionic nickel). In this way, the control layer was prepared. Following this, one side of the control layer was exposed to the aqueous solution of acrylamide (2.13 g) containing ammonium persulphate (0.07 g) and methylenebisacrylamide (2 wt%). Polymerization was then performed to acquire the substrate layer. The resulting reactor was profusely washed with ethanol and water, cut into pieces and then dried under flowing nitrogen.

Characterization: The TEM images of the prepared reactors were obtained using a transmission electron microscope (JEM-2100, Japan). The infrared spectra were recorded using a FTIR apparatus (Nicolet MX-1E, USA). The change in shape upon temperature was recorded with a digital camera, where the slice of reactors was taken out from hot water (40 °C, unless otherwise noted) and immediately snapped.

DLS: The DLS analysis was carried out using a Bettersize-2000 apparatus (China). In order to reach equilibrium, all samples were kept at specified temperatures for at least 10 min before acquiring the hydrodynamic radius (R_h). The relative change (R_c) of hydrodynamic radius reflecting the contribution of the PVIm-PAAc interaction was calculated as follows:

$$R_c = \left[\left(\frac{R_h - R_d}{R_d} \right)_S - \left(\frac{R_h - R_d}{R_d} \right)_N \right] \times 100\%$$

Herein, R_d is the particle size of the dried particles. S represents the smart catalytic reactors and N denotes the non-responsive reactor.

Catalysis Tests: The catalytic properties of the prepared reactors were evaluated in a batch format. Sodium fluorescein (SF) was added into a NaBH₄ aqueous solution with an initial concentration of $0.6 \times 10^{-2} \mu\text{mol mL}^{-1}$ (totally 4 mL; NaBH₄, tenfold with regard to SF). The solid content of reactors in the reaction system was 2.0 mg mL⁻¹. The reduction of SF was spectrophotometrically monitored. The catalytic activity of these reactors was obtained from the average of triple runs.

Electrochemical Tests: Using an electrochemical workstation (CHI760E, China), the Pt wire encircled by a thin film of the thermosensitive layer

(ca. 0.05 mm) was adopted as the working electrode in a three-electrode configuration (Au-plate counter electrode and Ag/AgCl ref. electrode). The redox process of $\text{HPO}_4^{2-}/\text{H}_2\text{PO}_4^-$ (PBS; pH 7.0) was used as a probe to achieve the current change upon changing temperature.

Acknowledgements

The authors want to express their gratitude to both Jiangsu Province and Jiangsu University for supporting this study under the distinguished professorship program (Sujiaoshi [2012]34 and No.12JG001) and the innovation/entrepreneurship program (Suzutong [2012]19). Thanks should be also expressed to the Science and Technology Agency of Jiangsu Province (BK20130486).

Received: March 8, 2014

Published online: May 23, 2014

-
- [1] F. H. Richter, Y. Meng, T. Klasen, L. Sahraoui, F. Schüth, *J. Catal.* **2013**, 308, 341–351.
- [2] W. G. Menezes, V. Zielasek, K. Thiel, A. Hartwig, M. Bäumer, *J. Catal.* **2013**, 299, 222–231.
- [3] C. W. Chen, M. Q. Chen, T. Serizawa, M. Akashi, *Adv. Mater.* **1998**, 10, 1122–1126.
- [4] Y. Lu, Y. Mei, M. Drechsler, M. Ballauff, *Angew. Chem. Int. Ed.* **2006**, 45, 813–816.
- [5] Y. Yang, X. Liu, X. Li, J. Zhao, S. Bai, J. Liu, Q. Yang, *Angew. Chem. Int. Ed.* **2012**, 51, 9164–9168.
- [6] T. Yang, J. Liu, Y. Zheng, M. J. Monteiro, S. Z. Qiao, *Chem. Eur. J.* **2013**, 19, 6942–6945.
- [7] L. Yang, M. Zhang, Y. Lan, W. Zhang, *New J. Chem.* **2010**, 34, 1355–1364.
- [8] T. Xie, *Polymer* **2011**, 52, 4985–5000.
- [9] B. C. Abberton, W. K. Liu, S. Keten, *J. Mech. Phys. Solids* **2013**, 61, 2625–2637.
- [10] J. Hu, Y. Zhu, H. Huang, J. Lu, *Prog. Polym. Sci.* **2012**, 37, 1720–1763.
- [11] Z. Hu, X. Zhang, Y. Li, *Science* **1995**, 269, 525–526.
- [12] Y. Li, Z. Hu, Y. Chen, *J. Appl. Polym. Sci.* **1997**, 63, 1173–1178.
- [13] A. Arslan, S. Kiralp, L. Toppare, A. Bozkurt, *Langmuir* **2006**, 22, 2912–2915.
- [14] A. Lendlein, S. Kelch, *Angew. Chem. Int. Ed.* **2002**, 41, 2034–2057.
- [15] W. Wang, X. Tian, Y. Feng, B. Cao, W. Yang, L. Zhang, *Ind. Eng. Chem. Res.* **2010**, 49, 1684–1690.
- [16] S. Li, Y. Ge, A. Tiwari, S. Cao, *Small* **2010**, 6, 2453–2459.
- [17] X. Wang, Y. Fu, *J. Phys. Chem. Solids* **2008**, 70, 192–196.
- [18] S. Li, Y. Luo, M. J. Whitcombe, S. A. Piletsky, *J. Mater. Chem. A* **2013**, 1, 15102–15109.
-